Original Article

DOI: 10.5582/ddt.2023.01100

Astragalus root increases Treg and Th17 involvement in embryo implantation and pregnancy maintenance by decreasing CTLA-4$^+$ Tregs

Kyoko Kobayashi*, Kenroh Sasaki

Division of Pharmacognosy, Faculty of Pharmaceutical Sciences, Tohoku Medical and Pharmaceutical University, Miyagi , Japan.

SUMMARY Maintenance of pregnancy is highly dependent on the maternal immune system. High levels of regulatory T cells (Tregs) accumulate in the maternal placenta to suppress immunoreactivity against fetal antigens. We assessed whether Astragalus root (AsR) and AsR-containing Kampo medicines modulate immunoreactivity and thereby increase mouse litter size. AsR-exposed murine splenocytes exhibited significantly increased IL-2 secretion. In AsR-exposed mice, total Tregs were significantly increased, whereas cytotoxic T lymphocyte antigen 4 (CTLA-4)-positive Tregs were decreased in AsR-exposed mice. Tregs express IL-2 receptor subunit alpha and are activated by IL-2. CTLA-4 interacts with B7 expressed in antigen-presenting cells (APCs) with high affinity, and CTLA-4/B7 signaling plays a critical role in inhibiting APC activity, thereby suppressing CD4$^+$ T cell proliferation and activation. The decrease in CTLA-4$^+$ Tregs in AsR-exposed mice is thought to induce an increase in CD4$^+$ T cells, leading to increased IL-2 secretion from CD4$^+$ T cells followed by Treg activation. Th17 cells prevent trophoblast apoptosis, resulting in trophoblast invasion into the decidua. AsR increases Th17 cells, thereby inducing dose-dependent increases in litter size. Although Keishikaogito (KO)- and Ogikenchuto (OK)-exposed mice exhibited increased IL-2 secretion and splenic Tregs, KO also increased CTLA-4$^+$ Tregs. Therefore, KO promoted immunosuppression by increasing CTLA-4$^+$ Tregs, which induced a decrease in Th17 and exerted little effect on litter size. Therefore, an increase in both Tregs and Th17 cells can be considered necessary for embryo implantation and pregnancy maintenance.

Keywords *Astragalus membranaceus*, Kampo medicine, IL-2, Treg/Th17, litter size

1. Introduction

Excessive immune responses to harmless environmental substances and self-antigens are known to cause autoimmune diseases, such as pollen allergy and inflammatory bowel disease. The proliferation and activation of regulatory T cells (Tregs) contribute to the suppression of immune responses against self-antigens, allergens, and allografts. Kakkonto, which has been used for the initial symptoms of colds such as chills, fever, and inflammatory congestive symptoms in the back and shoulder, was recently reported to induce immune tolerance (immunosuppression) against food antigens through the increase in Tregs in the intestinal mucosa (*1*). CD4$^+$ T cells differentiate into Th1, Th2, Th17, and Treg cells in response to T-cell receptor (TCR) stimulation by antigens presented on antigen-presenting cells (APCs). Tregs differentiated from CD4$^+$ T cells express abundant CD25 as the IL-2 receptor alpha chain and forkhead Box P3 (Foxp3) as the master transcription factor. CD4$^+$ CD25$^+$ Foxp3$^+$ Tregs are activated by IL-2 released from CD4$^+$ T cells and can generate an immunosuppressive microenvironment by secreting suppressive cytokines such as TGF-α and IL-10. Cytotoxic T-lymphocyte antigen 4 (CTLA-4) expressed on CD4$^+$ CD25$^+$ Foxp3$^+$ Tregs has the ability to suppress the maturation of APCs, by which Tregs bind to B7 (CD80/86) expressed on APCs. Tregs are classified into thymic-derived Tregs (tTregs) and peripheral-induced Tregs (pTregs) based on their origin. Leaving the thymus, tTregs migrate toward peripheral lymphoid tissues, *e.g.*, lymph nodes and spleen, and peripheral nonlymphoid tissues, such as intestinal mucosa, lung, liver, adipose tissue, infected tissues, grafts, placenta, and tumors (*2*). pTregs in the placenta are required for the maintenance of pregnancy stability. The maintenance of pregnancy is highly dependent on the maternal immune system against a semialleogenic fetus. In fact, pTreg-deficient mice have

been reported to raise the possibility of fetal resorption to the uterus (*3*), and it has also been reported that pTregs highly accumulate in the placenta of a maternal mouse, concomitant with an absolute decrease in circulating Tregs (*4*).

Weight loss in female athletes and excessive dieting lead to irregular menstruation, amenorrhea, and pregnancy failure because of homeostasis breakdown. Kampo medicines effectively improve immune system disorders, frailty, and irregular menstruation, which are difficult to treat with chemical drugs, by restoring and maintaining homeostasis. Astragalus root, the root of *Astragalus membranaceus*, has been used as a tonic mixed in Kampo medicines to modulate the immune system. We recently reported that the hot water extract of Astragalus root (AsR) increased blood estrogen levels in female mice and enhanced murine ovarian β-oxidation through the activation of PPARα (*5*). Furthermore, AsR increased the expression of Wnt/β-catenin signaling factors contributing to endometrial proliferation and decidual formation (*6*). Based on this background, we verified the possibility that AsR and AsR-containing Kampo medicines improve embryo implantation and fertility by enhancing maternal immune tolerance against the fetus.

2. Materials and Methods

2.1. Animals

Five-week-old SPF/BALB/c female mice (18-19 g, n = 96) and 7-week-old SPF/BALB/c male mice (22-23 g, n = 10) wern e purchased from Japan SLC Inc. (Shizuoka, Japan) and housed and maintained under standardized conditions of temperature (25 ± 1°C) and humidity (55 ± 5%) in a light cycle room (light from 07:00 a.m. to 07:00 p.m.; dark from 07:00 p.m. to 07:00 a.m.). The mice were fed standard chow (CE-2; CLEA Japan, Inc., Tokyo, Japan) and used for the experiment after being acclimatized to the room for one week. All experiments were approved by the Animal Experimental Committee of Tohoku Medical and Pharmaceutical University (approval No. 22044-cn), and the experimental procedures were conducted in accordance with the ethical guidelines of the university.

2.2. Extractions of samples

The dried, chopped crude drugs were purchased from Tochimoto Tenkaidou Co. Ltd. (Osaka, Japan). Five grams of Astragalus root, the root of *Astragalus mongholicus* or *A. membranaceus*, was boiled in 600 mL of distilled water to reduce the final volume by half. The boiled solution was filtered and concentrated in a rotary evaporator under reduced pressure at 50°C, and then the filtrate was freeze-dried to obtain AsR. The formulations of Japanese herbal medicines were prescribed as follows: Boiogito (Astragalus root, 5.0 g; Atractylodes rhizome, 3.0 g; Ginger, 1.0 g; Glycyrrhiza, 2.0 g, Jujube, 4.0 g; Sinomenium stem and rhizome, 4.0 g), Keishikaogito (Astragalus root, 3.0 g; Cinnamon bark, 3.0 g; Ginger, 1.0 g; Glycyrrhiza, 2.0 g; Jujube, 4.0 g; Peony root, 3.0 g), Kigikenchuto (Astragalus root, 2.0 g; Cinnamon bark, 4.0 g; Ginger, 1.0 g; Glycyrrhiza, 2.0 g; Japanese Angelica root, 4.0 g; Jujube, 4.0 g; Peony root, 5.0 g), Ogikenchuto (Astragalus root, 1.5 g; Cinnamon bark, 3.0 g; Ginger, 1.0 g; Glycyrrhiza, 3.0 g; Jujube, 3.0 g; Peony root, 6.0 g). Each formulation was boiled in 600 mL of distilled water to reduce the final volume by half. The decoctions were filtered and concentrated by a rotary evaporator under reduced pressure at 50°C and then freeze-dried to obtain the extracts of Boiogito (BO), Keishikaogito (KO), Kigikenchuto (KK) and Ogikenchuto (OK). The yields of extracts were measured to determine the dosages to mice.

2.3. WST-8 assay

Splenocyte proliferation was determined by using a WST-8 assay. BALB/c female mouse (n = 6) spleen was removed under sterile conditions after euthanasia by isoflurane anesthesia, minced in RPMI medium (RPMI-1640, FUJIFILM Wako Pure Chemical Corporation, Osaka, Japan), filtered through 40 μm mesh, and hemolyzed with red blood cell lysis buffer (pluriSelect Life Science, Leipzig, Germany). Splenocytes were suspended in RPMI medium containing 0.05 mM 2-mercaptoethanol (FUJIFILM Wako Pure Chemical Corporation), 10% heat-inactivated FBS (Gibco Fetal Bovine Serum, Qualified, ThermoFisher Scientific Inc, Tokyo Japan), antibiotic, and antimycotic (penicillin-streptomycin mixed stock solution, Nacalai Tesque Inc., Kyoto, Japan) and were adjusted to 5×10^4 viable cells per milliliter. Splenocyte suspension (100 μL) was seeded in each well of a 96-well plate and incubated with 10 μL of 0.4 mg/mL concanavalin A (concanavalin A from *Canavalia ensiformis*, Jack bean, Merck KGaA, Darmstadt, Germany) at 37°C in a humidified atmosphere containing 5% CO_2 for 24 h. Culture medium-dissolved test samples were added to each well. After 24 h of incubation, the cell count reagent (Cell Count Reagent SF, Nacalai Tesque Inc.) was added to each well and incubated for 4 h. Absorbance was measured at 450 nm with a reference wavelength of 600 nm using a microplate reader (SH-1300 microplate reader, Corona Electric Co., Ltd., Ibaraki, Japan).

2.4. IL-2 secretion test

Six-week-old female BALB/c mice (19-20 g, n = 4 in each group) were allowed free access to water solutions for 6 groups for 14 days: 0.8 (w/v) % AsR, 2.25 (w/v) % KO, 3.1 (w/v) % BO, 12.9 (w/v) % OK, and 3.0 (w/v) % KK, and control groups. After a 4-day

withdrawal of these solutions, 50 μg of concanavalin A (Concanavalin A from *Canavalia ensiformis*, Jack bean, Merck KGaA) suspended in 50 μL of complete Freund's adjuvant (Merck KGaA, Darmstadt, Germany) was injected subcutaneously through the tail to stimulate T cells. Seven days later, *i.e.*, 25 days after the start of sample administration, all mice (n = 24) were euthanasia by excessive inhalation of isoflurane. The spleen was extirpated under sterile conditions, minced in RPMI medium (RPMI-1640, FUJIFILM Wako Pure Chemical Corporation), filtered through 40 μm mesh and hemolyzed with red blood cell lysis buffer (pluriSelect Life Science). Splenocytes were suspended in RPMI medium containing 0.05 mM 2-mercaptoethanol (FUJIFILM Wako Pure Chemical Corporation), 10% heat-inactivated FBS (Gibco Fetal Bovine Serum, Qualified, ThermoFisher Scientific Inc), antibiotic and antimycotic (Penicillin-Streptomycin mixed stock solution, Nacalai Tesque Inc.) and were adjusted to 5 × 10^6 viable cells per milliliter. One milliliter of splenocyte suspension was seeded in each well of 24-well plates and incubated with 10 μL of 0.4 mg/mL concanavalin A (Concanavalin A from *Canavalia ensiformis*, Jack bean, Merck KGaA) at 37°C in a humidified atmosphere containing 5% CO_2. The medium was collected 18 h and 27 h after culture initiation, and the IL-2 concentrations in the medium were measured by ELISA (Mouse IL-2 Quantikine ELISA Kit, R&D Systems Inc., Minnesota, USA).

2.5. Flow cytometry

2.5.1. Sample preparation

Six-week-old female BALB/c mice (19-20 g, n = 6 in each group) were allowed free access to water solutions for 6 groups for 14 days: 0.8 (w/v) % AsR, 2.25 (w/v) % KO, 3.1 (w/v) % BO, 12.9 (w/v) % OK, and 3.0 (w/v) % KK, and control groups. Astragaloside IV (Biosynth Ltd., Staad, Switzerland), and formononetin (Tokyo Chemical Industry Co. Ltd., Tokyo, Japan) were subcutaneously injected once a day at 10 mL/kg for 14 days. After a 4-day withdrawal of these solutions, 50 μg concanavalin A suspended in 50 μL complete Freund's adjuvant (Merck KGaA) was injected subcutaneously through the tail to stimulate T cells. Seven days later, *i.e.*, 25 days after the start of sample administration, all mice (n = 36) were euthanasia by excessive inhalation of isoflurane. The spleen was extirpated under sterile conditions, minced in RPMI medium (RPMI-1640, FUJIFILM Wako Pure Chemical Corporation), filtered through 40 μm mesh and hemolyzed with red blood cell lysis buffer (pluriSelect Life Science) to prepare splenocytes.

2.5.2. Cell staining and flow cytometric analysis

Before cell staining, splenocytes were fixed and permeabilized by Fixation/Permeabilization solution (Fixation/Permeabilization Concentrate and Diluent, ThermoFisher Scientific Inc.). Then, splenocytes suspended in 400 μL buffer were divided 100 μL into 4 tubes (A~D). For analysis of $CD4^+$ T cells, splenocytes in tube B were stained with Super Bright 600-labeled CD4 antibody. For analysis of Treg, IL-10^+ Treg, and CTLA-4^+ Treg cells in tube C were stained with Super Bright 600-labeled CD4 antibody, PE-Cyanine 5-labeled CD25 antibody, PE-labeled CD152 antibody, Alexa Fluor 700-labeled IL-10 antibody and Alexa Fluor 488-labeled Foxp3 antibody. For analysis of Th17 cells, splenocytes in tube D were stained with Super Bright 600-labeled CD4 antibody and eFluor 450-labeled IL-17A antibody. All antibodies for cell-staining were purchased from ThermoFisher Scientific Inc. Splenocytes in tube A were not stained with antibodies. After adding the antibodies, splenocytes in tubes B, C, and D were incubated on ice for 1 hour and then washed once with PBS. Measurements by flow cytometry of splenocytes in tubes A, B, C, and D were performed on an Attune NxT Acoustic Focusing Cytometer (Thermo Fisher Scientific Inc.), and these data were collected and analyzed by Attune NxT Software (Thermo Fisher Scientific Inc.).

2.6. Mating test

Six-week-old female BALB/c mice (18-19 g, n = 6 per group) were free-accessed to water solutions for 5 groups for 14 days: 0.4 and 0.8 (w/v) % AsR and 1.125 and 2.25 (w/v) % KO, and control groups. Then, 3 female mice per 10-week-old BALB/c male mouse were mated in the same cage. Pregnancy was assessed by their appearance and body weight gain from the mating day. Approximately 3 days before parturition, pregnant mice were housed singly. Three days after parturition, the number of neonatal mice per maternal mouse was counted as the litter size.

2.7. Statistical analysis

All data are expressed as the mean values ± standard deviations (SD). Comparisons among the means were performed using Sigma Stat statistical software ver. 2.03 (SPSS, Inc., CA, USA): Student's unpaired t test or one-way ANOVA followed by Dunnett's multiple comparison test was performed for comparisons against a control group. Statistical significance was set at $P < 0.05$.

3. Results

3.1. Splenocyte proliferation evaluation and IL-2 secretion

To determine whether splenocyte proliferation was induced or inhibited, splenocytes harvested from female BALB/c mice were exposed to AsR, KO, BO,

OK, or KK. Compared with the control (100% of cell proliferation), AsR-treated splenocytes exhibited a substantial increase, and did not inhibit over the measured reaction concentration range (Figure 1A). KO-exposed splenocytes tended to exhibit increased cell proliferation, and the highest reaction concentrations of KO showed no increase in cell proliferation from the initial cell number. As shown in Figure 1B, BO, OK, and KK showed no increase in cell proliferation, but decreased cell proliferation at higher concentrations.

To determine whether IL-2, which is essential for Treg activation, was increased by AsR, KO, BO, OK, and KK extract, splenocytes harvested from female BALB/c mice were cultured. AsR-exposed mice showed significantly increased IL-2 secretion at 18 and 27 h after culture initiation, whereas KO- and OK-exposed mice showed significantly increased IL-2 secretion at 27 h (Figure 1C).

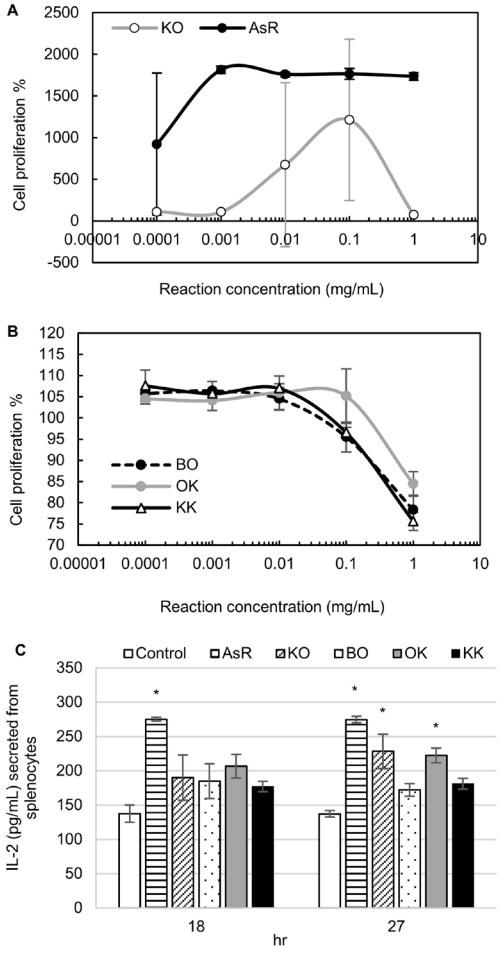

Figure 1. Effects of Astragalus root (AsR) and AsR-containing Kampo medicine exposure on splenocyte proliferation and IL-2 secretion from cultivated splenocytes. Splenocyte proliferation and IL-2 secretion levels from the splenocytes of AsR-, KO-, BO-, OK-, and KK-exposed female mice were compared with those in control mice. AsR-exposed splenocytes demonstrated dramatic increases in cell proliferation at 0.001-1.0 mg/mL, while KO-exposed splenocytes exhibited increased cell proliferation at 0.01-0.1 mg/mL (**A**). BO-, OK-, and KK-exposed splenocytes decreased cell proliferation at 1.0 mg/mL (**B**). AsR-exposed mice showed significantly increased IL-2 secretion levels from cultured splenocytes at 18 and 27 h of incubation, and KO and OK-exposed mice showed significantly increased IL-2 secretion levels at 27 h (**C**). AsR, Astragalus root; KO, Keishikaogito; BO, Boiogito; OK, Ogikenchuto; KK, Kigikenchuto. One-way ANOVA was used for data analysis, followed by Dunnett's multiple comparison test; $*P < 0.05$. The bar graphs and error bars represent the means ± SDs ($n = 4$).

3.2. Evaluation of splenic Treg and Th17 on AsR-exposed mice

To determine whether Tregs essential for accepting an allogeneic fetus to the decidua were induced by AsR, splenic Tregs were measured *via* flow cytometry analysis. After measuring the percentage of $CD4^+$ T cells in the splenic lymphocyte population, the percentage of $CD25^+$ $Foxp3^+$ T cells in the $CD4^+$ T-cell population was measured. Tregs were defined as $CD4^+$ $CD25^+$ $Foxp3^+$ T cells. Representative flow cytometry dot plots show gating (right upper quadrant) for $CD25^+$ $Foxp3^+$ T cells in $CD4^+$ T cells (Figure 2A). Compared with the control group, the AsR-administered mice had a significantly increased percentage of Tregs among $CD4^+$ T cells (Figure 2B).

To determine whether AsR generates an immunosuppressive environment by increasing the suppressive cytokine IL-10, splenic $IL\text{-}10^+$ Tregs were measured *via* flow cytometry analysis. After measuring the percentage of $CD4^+$ T cells in the splenic lymphocyte population, the percentage of $IL\text{-}10^+$ $Foxp3^+$ T cells was measured. $IL\text{-}10^+$ Tregs were defined as $CD4^+$ $IL\text{-}10^+$ $Foxp3^+$ T cells. Representative flow cytometry dot plots show gating (right upper quadrant) for $IL\text{-}10^+$ $Foxp3^+$ T cells in $CD4^+$ T cells (Figure 2A). Compared with the control group, $IL\text{-}10^+$ Tregs were significantly increased in AsR-administered mice (Figure 2C). To determine whether Th17 cells essential for promoting trophoblast invasion into decidua were induced by AsR, splenic Th17 cells were measured *via* flow cytometry analysis. After measuring the percentage of $CD4^+$ T cells in the splenic lymphocyte population, the percentage of $CD4^+$ $IL\text{-}17A^+$ T cells in $CD4^+$ T cells was measured. Th17 cells were defined as $CD4^+$ $IL\text{-}17A^+$ T cells. Representative flow cytometry dot plots show gating (right upper quadrant) for $CD4^+$ $IL\text{-}17A^+$ T cells in $CD4^+$ T cells (Figure 2D). Compared with the control group, AsR-exposed mice had a significantly increased percentage of Th17 cells among $CD4^+$ T cells (Figure 2E). An imbalance in the Treg/Th17 ratio has been observed in patients with recurrent spontaneous abortion. AsR-exposed mice showed no difference in the ratio compared with that of control mice (Figure 2F).

CTLA-4, known as CD152 expressed on Tregs, has the ability to strip off B7 (CD80/CD86) from APCs and impair the antigen-presenting activity of APCs, which leads to immunosuppression. To determine whether the expression of CTLA-4 on Tregs was increased or decreased by AsR, splenic $CTLA\text{-}4^+$ Tregs were

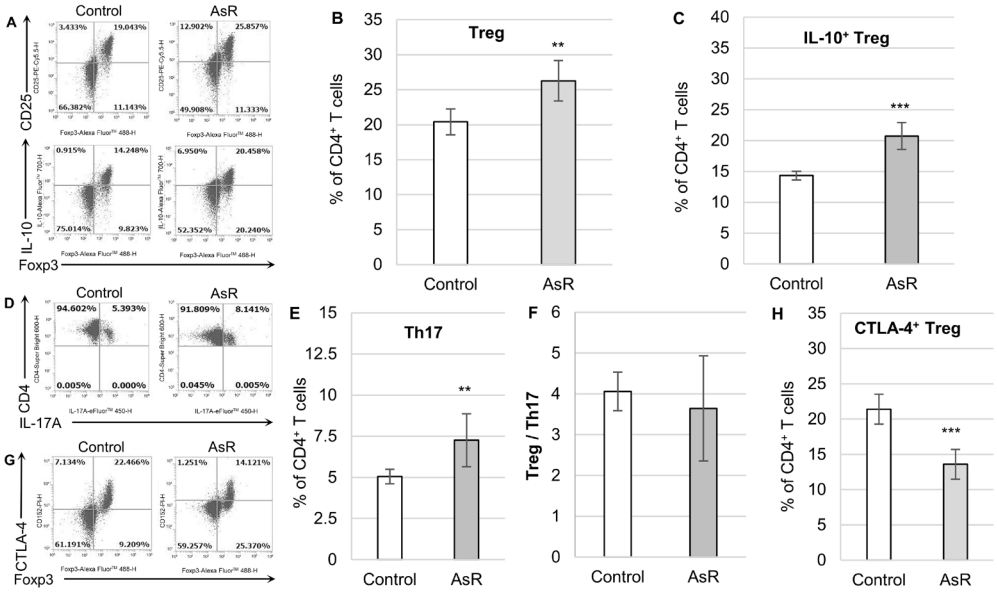

Figure 2. Effect of Astragalus root (AsR) exposure on splenic Tregs, IL-10$^+$ Tregs, Th17, Treg/Th17 ratio, and CTLA-4$^+$ Tregs. Tregs, IL-10$^+$ Tregs, Th17 cells, Treg/Th17 ratio, and CTLA-4$^+$ Tregs in CD4$^+$ lymphocytes of splenocytes prepared from AsR-exposed BALB/c female mice. Representative flow cytometric analysis of Tregs and IL-10$^+$ Tregs (**A**, CD25$^+$ Foxp3$^+$ T cells, or IL-10$^+$ Foxp3$^+$ T cells in CD4$^+$ T cells, right upper quadrant) in AsR-exposed and control mice. AsR-treated mice showed significantly increased Treg (**B**) and IL-10$^+$ Treg levels (**C**). Representative flow cytometric analysis of Th17 (**D**, IL-17$^+$ T cells in CD4$^+$ T cells, right upper quadrant) in AsR-exposed and control mice. AsR-exposed mice show an increased number of Th17 cells (**E**). The Treg/Th17 ratio was not significantly different (**F**). Representative flow cytometric analysis of CTLA-4$^+$ Tregs (**G**, Foxp3$^+$ CTLA-4$^+$ T cells in CD4$^+$ T cells, right upper quadrant) of AsR-treated and control mice. AsR-treated mice showed significantly decreased levels of CTLA-4$^+$ Tregs (**H**). AsR, Astragalus root. Student's *t* test was used for data analysis; $^{**}P < 0.01$, and $^{***}P < 0.001$. The bar graphs and error bars represent the means ± SDs ($n = 6$).

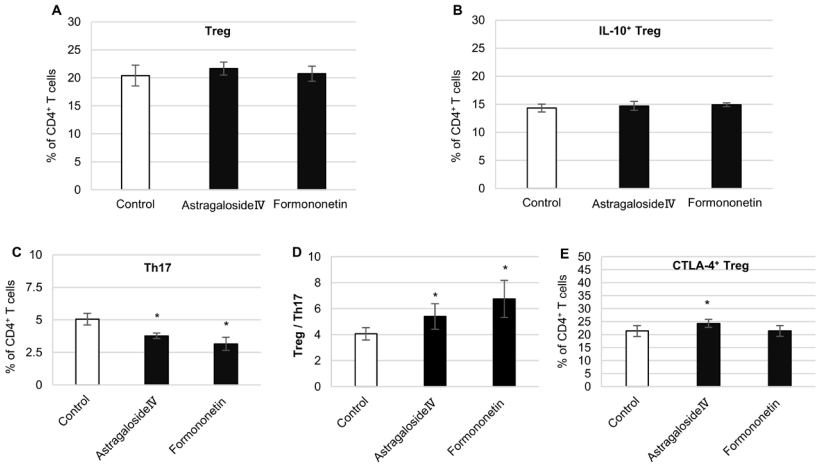

Figure 3. Effects of astragaloside IV and formononetin on splenic Tregs, IL-10$^+$ Tregs, Th17 cells, Treg/Th17 ratio, and CTLA-4$^+$ Tregs in mice. Treg (**A**), IL-10$^+$ Treg (**B**), and Th17 (**C**) in CD4$^+$ lymphocytes in splenocytes prepared from astragaloside IV- and formononetin-exposed BALB/c female mice. Astragaloside IV- and formononetin-exposed mice had a significantly decreased Th17 compared with control mice, thereby increasing the Treg/Th17 ratio (**D**). Astragaloside IV-exposed mice had a significantly increased CTLA-4$^+$ Treg (**E**). One-way ANOVA was used for data analysis, followed by Dunnett's multiple comparison test; $^{*}P < 0.05$. The bar graphs and error bars represent the means ± SDs ($n = 6$).

measured *via* flow cytometry analysis. After measuring the percentage of CD4$^+$ T cells in the splenic lymphocyte population, the percentage of CTLA-4$^+$ Foxp3$^+$ T cells in the CD4$^+$ T-cell population was measured. CTLA-4$^+$ Tregs were defined as CD4$^+$ Foxp3$^+$ CTLA-4$^+$ T cells. Representative flow cytometry dot plots show gating (right upper quadrant) for CTLA-4$^+$ Tregs (Figure 2G). AsR-exposed mice had significantly decreased CTLA-4$^+$ Tregs (Figure 2H).

3.3. Evaluation of splenic Treg and Th17 on formononetin and astragaloside IV-exposed mice

Formononetin (an isoflavone molecule) and astragaloside IV (a triterpene glucoside) contained in Astragalus roots were the main compounds that had no effect on the percentage of Tregs (Figure 3A) and IL-10$^+$ Tregs in CD4$^+$ T cells (Figure 3B). On the other hand, formononetin and astragaloside IV significantly

decreased the percentage of Th17 cells among $CD4^+$ T cells (Figure 3C), and thus significantly increased the Treg/Th17 ratio (Figure 3D) relative to that of the control. Furthermore, astragaloside IV-exposed mice showed a significant increase in CTLA-4^+ Tregs (Figure 3E).

3.4. Evaluation of splenic Treg and Th17 on AsR-containing Kampo medicines-exposed mice

To determine whether Kampo medicines containing Astragalus root used for the treatment of frail conditions increase splenic Treg, KO-, BO-, OK-, and KK-exposed mice were measured for the percentage of Treg in $CD4^+$ T cells *via* flow cytometry analysis. Representative flow cytometry dot plots show gating (right upper quadrant) for $CD25^+$ $Foxp3^+$ Tregs in $CD4^+$ T cells (Figure 4A). KO-, OK-, and KK-exposed mice had significantly more Tregs (Figure 4B) than control mice. KO-, BO-, OK-, and KK-exposed mice were measured for IL-10^+ Tregs in $CD4^+$ T cells *via* flow cytometry analysis. Representative flow cytometry dot plots show gating (right upper quadrant) for IL-10^+ Tregs in $CD4^+$ T cells (Figure 4A). KO-, BO-, and OK-exposed mice had significantly increased IL-10^+ Tregs (Figure 4C) relative to control mice. KO-, BO-, OK-, and KK-exposed mice were measured for the percentage of Th17 cells among $CD4^+$ T cells *via* flow cytometry analysis. Representative flow cytometry dot plots show gating (right upper quadrant) for $CD4^+$ IL-$17A^+$ T cells in $CD4^+$ T cells (Figure 4D). KO-exposed mice had a significantly decreased percentage of Th17 cells among $CD4^+$ T cells (Figure 4E) relative to control mice. KO-, and OK-exposed mice significantly increased the Treg/Th17 ratio (Figure 4F).

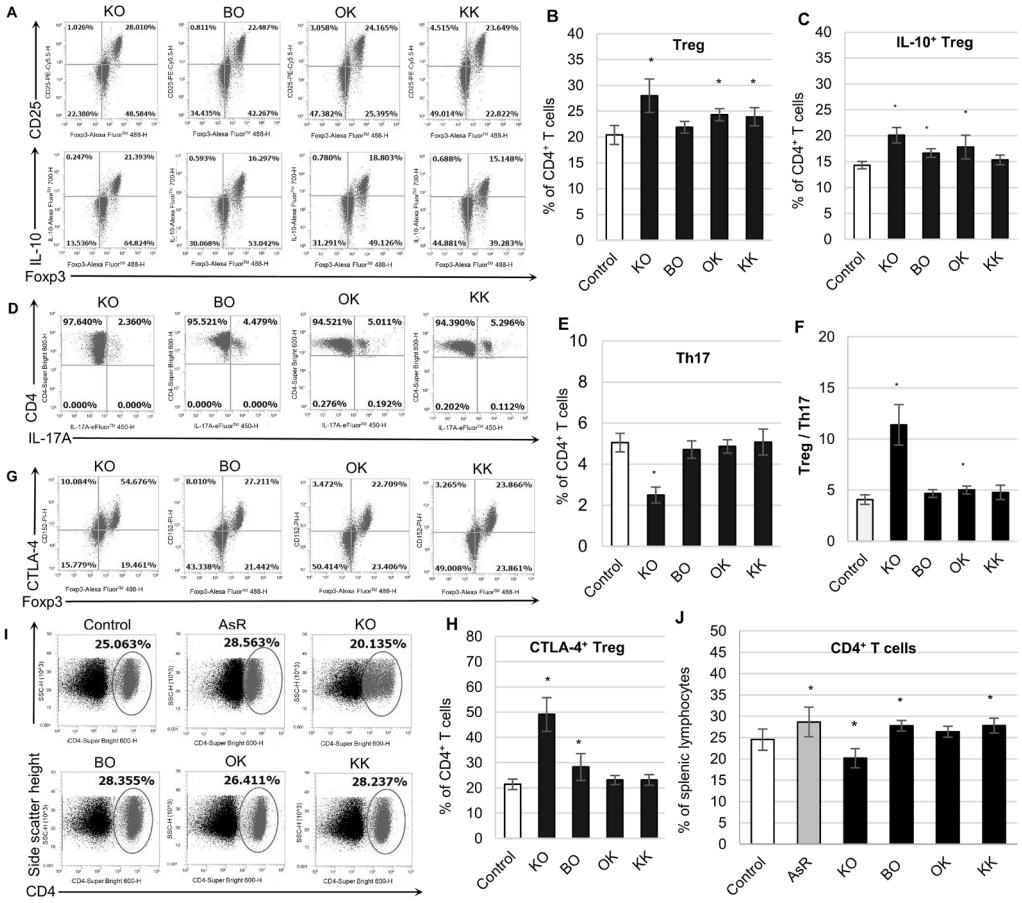

Figure 4. Effects of AsR-containing Kampo medicines exposure on splenic Tregs, IL-10^+ Tregs, Th17, Treg/Th17 ratio, CTLA-4^+ Tregs, and $CD4^+$ T cells. The Treg, IL-10^+ Treg, Th17, Treg/Th17 ratio, and CTLA-4^+ Treg in $CD4^+$ lymphocytes of splenocytes prepared from KO-, BO-, OK-, and KK-exposed BALB/c female mice. Representative flow cytometric analysis of Tregs and IL-10^+ Tregs (**A**, $CD25^+$ $Foxp3^+$ T cells, or IL-10^+ $Foxp3^+$ T cells in $CD4^+$ T cells, right upper quadrant) in KO-, BO-, OK-, KK-exposed and control mice. KO-, OK-, and KK-treated mice showed significantly increased Treg levels (**B**). KO-, BO-, and OK- treated mice showed significantly increased IL-10^+ Tregs (**C**). Representative flow cytometric analysis of Th17 (**D**, IL-17^+ T cells in $CD4^+$ T cells, right upper quadrant) in KO, BO, OK, KK-exposed and control mice. KO-exposed mice showed significantly decreased Th17 levels (**E**). KO and OK-exposed mice showed a significantly increased Treg/Th17 ratio (**F**). Representative flow cytometric analysis in CTLA-4^+ Treg (**G**, CTLA-4^+ $Foxp3^+$ T cells in $CD4^+$ T cells, right upper quadrant) of KO, BO, OK, KK-exposed and control mice. KO- and BO-exposed mice showed significantly increased CTLA-4^+ Tregs (**H).** Representative flow cytometric analysis of $CD4^+$ T cells in lymphocytes (**I**, circle) of AsR, KO, BO, OK, KK-exposed and control mice. AsR-, BO-, and KK-exposed mice showed significantly increased $CD4^+$ T cells, and KO-exposed mice showed a significant decrease in $CD4^+$ T cells **(J)**. KO, Keishikaogito; BO, Boiogito; OK, Ogikenchuto; KK, Kigikenchuto. One-way ANOVA was used for data analysis, followed by Dunnett's multiple comparison test; $*P < 0.05$. The bar graphs and error bars represent the means ± SDs ($n = 6$).

KO-, BO-, OK-, and KK-exposed mice were measured for the percentage of CTLA-4$^+$ Tregs in CD4$^+$ T cells *via* flow cytometry analysis. Representative flow cytometry dot plots show gating (right upper quadrant) for CTLA-4$^+$ Tregs (Figure 4G). Compared with the control group, KO- and BO-exposed mice had an increased percentage of CTLA-4$^+$ Tregs (Figure 4H), particularly KO-exposed mice, which showed an approximately 2-fold increase relative to the control.

3.5. Evaluation of splenic CD4$^+$ T cells

To determine whether the increase in CTLA-4$^+$ Tregs leads to a decrease in CD4$^+$ T cells, CD4$^+$ T cells in the splenic lymphocyte population were measured *via* flow cytometry analysis. Representative flow cytometry dot plots show gating (circle) for CD4$^+$ T cells (Figure 4I). KO-exposed mice significantly decreased the percentage of CD4$^+$ T cells in the splenic lymphocyte population, and AsR-, BO-, and KK-exposed mice significantly increased the percentage of CD4$^+$ T cells (Figure 4J).

3.6. Assessment of pregnancy

To determine whether fertility depends on the Treg/Th17 rate, AsR- and KO-exposed BALB/c mice were assessed with the average number of litters. The number of litters per maternal mouse was measured 4 days postpartum. AsR-exposed mice, which had no difference in Treg/Th17 compared with control mice, showed a trend toward a dose-dependent increase in the average number of litters (Figure 5A). KO-exposed mice, which had a significantly increased Treg/Th17 rate, showed no increase in the average number of litters compared with the control group (Figure 5B).

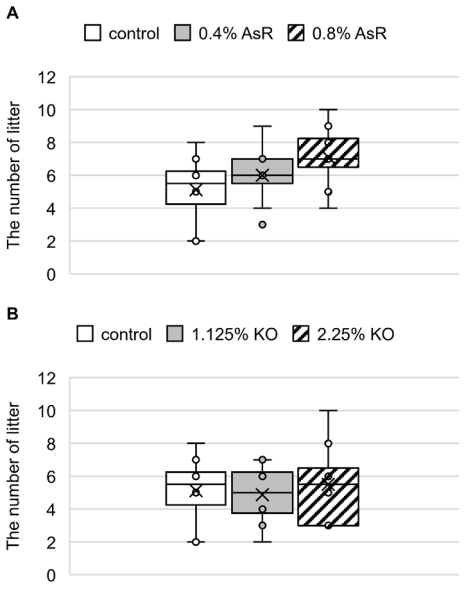

Figure 5. Effect of AsR and KO on the number of litters. A box-whisker plot was applied to indicate the number of litters. AsR-exposed mice showed a trend toward a dose-dependent increase in the average number of litters (**A**), whereas KO-exposed mice did not (**B**). The average number of litter was presented by "×" (n = 8). The number of litter in each maternal mouse was presented by "○" and "the ends of the whiskers". The lower and upper edges of the box signal the 25th percentile and 75th percentile, respectively. The parallel line across the box indicates the median of the distribution. AsR, Astragalus root; KO, Keishikaogito.

4. Discussion

The present study shows that AsR, which is used as a tonic contained in Kampo medicines, has the ability to promote embryo implantation and maintain pregnancy by improving the immune system. AsR further increased concanavalin A-enhanced splenocyte proliferation (Figure 1A). Kampo medicines, except KO, demonstrated no increase in cell proliferation (Figure 1B), suggesting that AsR and KO may promote T cell immunostimulation. IL-2 is secreted from antigen-activated CD4$^+$ helper T cells and consumed to activate Tregs and convert naïve CD8$^+$ T cells to effector CD8$^+$ T cells (*7*). Therefore, IL-2 is currently used to suppress immune responses in patients with autoimmune diseases and to enhance immune responses in patients with cancer and HIV-infected diseases. The administered dose of AsR (0.8% AsR-containing water solution, free access for 14 days) in this study was determined by the yield of the extract. In Figure 1C, cultured splenocytes of AsR-administered mice showed a significant increase in IL-2 secretion at 18 h and 27 h from incubation initiation. Therefore, AsR was thought to contribute to the activation of CD4$^+$ T cells.

In the secondary lymphoid tissue (spleen, lymph nodes), the CD4$^+$ T-cell subset comprises 10-15% of the Treg subset. CD4$^+$ Foxp3$^-$ T cells circulating in secondary lymphoid tissues are differentiated by IL-2 into CD4$^+$ Foxp3$^+$ Tregs, which accumulate in peripheral nonlymphoid tissue. Tregs are potent suppressors of inflammatory effector T cells, such as CD8$^+$ T cells, conventional CD4$^+$ T cells, and NK cells. It is well established that lymphocytes migrate into the maternal endometrium during the luteal phase and pregnancy (*8*), and Tregs particularly increase in the decidua during the first and second trimesters of pregnancy (*4*). Tregs in mice increase during the estrous cycle and early pregnancy (*9*). As shown in Figure 2B, Treg in splenic lymphocytes was significantly increased in AsR-administered mice, and thus AsR might increase the migrated number of Treg to peripheral nonlymphoid tissue, such as decidua, from the spleen.

Maternal immune tolerance induced by Tregs is essential for accepting fetal antigens to the decidua. CTLA-4, known as CD152, is a cell surface molecule constitutively expressed in Foxp3$^+$ Tregs but absent in naïve conventional T cells. CTLA-4 has a high affinity for B7 expressed in APCs, and CTLA-4/B7 signaling plays a critical role in inhibiting the activity of APCs, thereby suppressing the proliferation and activation of T

cells and the production of cytokines. It was reported that blocking the interaction of CTLA-4/B7 increases T-cell proliferation and IL-2 production (*10*). Furthermore, the blockade of CTLA-4 by ligands increases Tregs due to increased IL-2 production from $CD4^+$ T cells through enhanced CD28/B7 signaling (*11*). CTLA-4-Ig gene transfer-model mice have decreased embryonic absorption rates and improved recurrent pregnancy loss in association with increased levels of peripheral Treg (*12*). CTLA-4^+ Tregs were decreased in AsR-administered mice (Figure 2H), leading to an increase in the percentage of $CD4^+$ T cells in the splenic lymphocyte population (Figure 4J). These findings suggest a mechanism of AsR, as shown in Figure 6.

The trophoblast cells anchoring the placenta to the uterine wall in mice express indoleamine 2,3-dioxygenase (IDO), which mediates tryptophan catabolism into kynurenine, which drives Treg expansion. Lower IDO levels in mice have been reported to induce pregnancy loss associated with a lower number of splenic Tregs in maternal mice (*13-15*). Tregs recognize inflammatory effector cells, such as $CD8^+$ cytotoxic T cells (CTLs), $CD4^+$ T cells, and NK cells which attack fetal antigens in the murine endometrium. Th17 cells, which produce the proinflammatory cytokine IL-17, play a crucial role in the induction of autoimmune diseases such as rheumatoid arthritis, and an imbalance in Th17/Treg cells was observed in patients with recurrent spontaneous abortion. However, Th17 cells promote the proliferation and invasion of human trophoblasts into the maternal decidua (invaded trophoblasts named extravillous trophoblast cells: EVTs), and IL-17 excludes other cytokines and prevents apoptosis of EVTs (*8*). Murine trophoblasts (trophoblast giant cells and glycogen trophoblasts) are modestly more invasive than human trophoblasts. AsR increased peripheral Th17 (Figure 2E) and the number of litters in an AsR dose-dependent manner (Figure 5A), which suggests that AsR prevents trophoblast apoptosis.

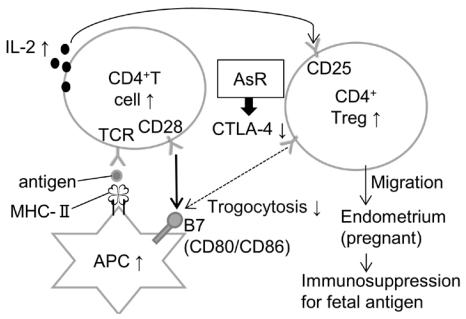

Figure 6. AsR-induced immunosuppressive milieu in splenic lymphocytes. AsR leads to APC activation by attenuated expression of CTLA-4 on Tregs. $CD4^+$ T cells increased by APC activation secrete IL-2, which binds to CD25 to activate Tregs, creating an immunosuppressive milieu. AsR, Astragalus root; APC, antigen-presenting cells; CTLA-4, cytotoxic T lymphocyte antigen 4; Treg, regulatory T cells; TCR, T-cell receptor; MHC-II, major histocompatibility complex II.

Formononetin, an isoflavone molecule contained in the Astragalus root, shows a wide range of pharmacological activities, such as anti-inflammatory (*16*), antidiabetic (*17*), neuroprotective (*18*), and cerebral anti-ischemia (*19*) activities. In this study, formononetin decreased splenic Th17 cells (Figure 3C) but had no effect on Tregs. Formononetin inhibits the activation of STAT3 (*20*), a Th17 transcription factor. Formononetin-administered BALB/c mice appeared to inhibit the activation of nuclear factor kappa β (NF-kB) related to the IL-17 signaling pathway (*21*). Astragaloside IV, a triterpene glucoside contained in AsR, plays important roles in the improvement of the immune system to suppress the migration of cervical cancer cells (*22*) and type 2 diabetes mellitus to prevent mitochondrial dysfunction (*23*). Astragaloside IV decreases IL-6 secretion from dendritic cells (DCs), which downregulates Th17 differentiation from $CD4^+$ T cells (*24*). In this study, astragaloside IV showed a significant increase in CTLA4^+ Tregs (Figure 3E) and a significant decrease in Th17 cells (Figure 3C). Astragalus polysaccharide (ASP) is an immunoreactive molecule, and ASP-treated DCs displayed mature morphology and augmented the cell surface expression of MHC-II (*25*). ASP decreases CTLA-4 mRNA expression and increases IL-2 mRNA expression (*26*). In our study, ASP was significantly decreased in murine splenic $CD4^+$ CTLA-4^+ T cells (data not shown, $P < 0.01$, *t* test) but did not decrease in CTLA-4^+ Tregs. Blockage of CTLA-4 on $CD4^+$ T cells promotes the proliferation of $CD4^+$ cells more than $CD8^+$ cells (*27*). We found no components in AsR that showed a mechanism in a manner similar to AsR for increasing Tregs.

To evaluate whether AsR-containing Kampo medicines (KO, BO, OK, KK) show a mechanism similar to that of AsR the percentages of Tregs, IL-10^+ Tregs, CTLA-4^+ Tregs, and Th17 cells in $CD4^+$ lymphocytes were measured. KO-administered mice exhibited the most strongly enhanced percentage of splenic Tregs (Figure 4B). KO-administered mice had increased IL-10^+ Tregs (Figure 4C) and decreased splenic Th17 cells (Figure 4E). The percentages of splenic CTLA-4^+ Tregs were dramatically increased in the spleens of KO-administered mice (Figure 4H). CTLA-4 expressed on Tregs has the ability to strip off MHC-II and the costimulatory molecule B7 from APCs and express B7 on the surface of CTLA-4^+ Tregs, resulting in impaired antigen-presenting activity of APCs (*28*). KO was thought to strongly induce this 'trogocytosis' by the overexpression of CTLA-4 on Tregs, resulting in a decrease in the percentage of $CD4^+$ T cells in the splenic lymphocyte population (Figure 4J).

Disruption of maternal-fetal immune balance, especially Treg/Th17 imbalance, is linked to recurrent spontaneous abortion (RSA). The immunosuppressant cyclosporine A, which is used for the treatment of RSA (*29*), improves the Treg/Th17 imbalance in RSA patients

(increased Th17 and decreased Treg compared with normal early pregnancy) and increases the live birth rate (*30*). To determine whether Treg/Th17 imbalance impacts pregnancy, the number of litters in AsR- and KO-exposed female mice was investigated. The number of litters showed a trend toward a dose-dependent increase in AsR-administered mice (Figure 5A) but did not increase in KO-administered mice (Figure 5B). AsR increased the percentage of both Treg and Th17 cells through a decrease in CTLA-4 expression on Treg cells and did not exhibit a Treg/Th17 imbalance, which could be one reason for the decreased litter size. AsR was thought to create an environment of immunosuppression and easy trophoblast proliferation in the endometrium to improve embryo implantation.

Multicomponent drugs, such as crude drugs and herbal medicines, have multiple targets in several signaling pathways, and it is difficult to identify their potential targets. The Network Pharmacology approach is effective in predicting all the main active ingredients of multicomponent drugs against the core targets of the disease. The seven ingredients, including formononetin, contained in the mixture of *Astragalus membranaceus* and *Angelica sinensis* were predicted to influence the core targets in the Toll-like receptor, IL-17, and TNF signaling pathways in atherosclerosis (*31*). Furthermore, the combination of *A. membranaceus* and *Ligusticum chuanxiong* treatment predicted that 14 components of *A. membranaceus* including formononetin, activated the core targets of three pathways in ischemic stroke: the Toll-like receptor, IL-17, and TNF signaling pathways (*32*). In addition, Buyang Huanwu's decoction containing *A. membranaceus* predicted that the quercetin content is linked to the core targets of the Il-17 signaling pathway in myocardial fibroblast, and *in vivo* assays revealed increased IL-6, IL-1β, and MMP expression in the IL-17 signaling pathway (*33*). *A. membranaceus* was significantly increased in splenic Th17. Conclusively, these findings suggest that the components of *A. membranaceus* may compositely activate the IL-17 pathway to improve embryo implantation.

The present research shows that AsR exposure improves embryo implantation and maintaining pregnancy and suggests a mechanism that involves enhanced maternal-fetal immune tolerance through increased Treg and Th17 numbers in splenic lymphocytes. Immune tolerance due to a decrease in T cells mediated by an increase in CTLA-4 on Tregs is thought to adversely affect maintaining pregnancy. Therefore, to create an immune tolerance milieu of peripheral nonlymphoid tissues such as the uterine mucosa, it would be worth considering ways to increase the number of immune cells in peripheral lymphoid tissue and promote Treg migration to peripheral nonlymphoid tissues. Specific microRNA expression is correlated with endometrium decidualization and trophoblast cell proliferation in the placenta during pregnancy (*34*). We would like to investigate the correlation between Treg, Th17, and the microRNA expression levels in decidua and further clarify the mechanism of maintaining pregnancy.

Acknowledgements

The authors would like to thank Yukie Sato for technical assistance with the experiments.

Funding: This work was supported by JSPS KAKENHI Grant Number JP20K07856. .

Conflict of Interest: The authors have no conflicts of interest to disclose.

References

1. Nagata Y, Yamamoto T, Hayashi M, Hayashi S, Kadowaki M. Improvement of therapeutic efficacy of oral immunotherapy in combination with regulatory T cell-inducer Kakkonto in a murine food allergy model. PLoS ONE. 2017; 12:e0170577.
2. Richards DM, Delacher M, Goldfarb Y, Kägebein D, Hofer AC, Abramson J, Feuerer M. Treg cell differentiation: From thymus to peripheral tissue. Prog Mol Biol Transl Sci. 2015; 136:175-205.
3. Samstein RM, Josefowicz SZ, Arvey A, Treuting PM, Rudensky AY. Extrathymic generation of regulatory T cells in placental mammals mitigates maternal-fetal conflict. Cell. 2012; 150:29-38.
4. Tsuda S, Nakashima A, Morita K, Shima T, Yoneda S, Kishi H, Saito S. The role of decidual regulatory T cells in the induction and maintenance of fetal antigen-specific tolerance: Imbalance between regulatory and cytotoxic T cells in pregnancy complications. Hum Immunol. 2021; 82:346-352.
5. Orkhon B, Kobayashi K, Javzan B, Sasaki K. Astragalus root induces ovarian β-oxidation and suppresses estrogen-dependent uterine proliferation. Mol Med Rep. 2018; 18:5198-5206.
6. Kobayashi K, Sasaki K. Investigation of murine fertility by Kampo formula containing Astragalus root enhanced endometrial Wnt/β-catenin signaling factors. Int J Pharmacogn Chinese Med. 2020; 4:000195.
7. Chinen T, Kannan AK, Levine AG, Fan X, Klein U, Zheng Y, Gasteiger G, Feng Y, Fontenot JD, Rudensky AY. An essential role for IL-2 receptor in regulatory T cell function. Nat Immunol. 2016; 17:1322-1333.
8. Wu HX, Jin LP, Xu B, Liang SS, Li DJ. Decidual stromal cells recruit Th17 cells into decidua to promote proliferation and invasion of human trophoblast cells by secreting IL-17. Cel Mol Immunol. 2014; 11:253-262.
9. Thaxton JE, Sharma S. Interleukin-10: A multi-faceted agent of pregnancy. Am J Reprod Immunol. 2010; 63:482-491.
10. McCoy KD, Gros GL. The role of CTLA-4 in the regulation of T cell immune responses. Immunol Cell Biol. 1999; 77:1-10.
11. Schubert D, Bode C, Kenefeck R *et al*. Autosomal dominant immune dysregulation syndrome in humans with CTLA4 mutations. Nat Med. 2014; 20:1410-1416.

12. Li W, Li B, Fan W, Geng L, Li X, Li L, Hang Z, Li S. CTLA4Ig gene transfer alleviates abortion in mice by expanding $CD4^+$ $CD25^+$ regulatory T cells and inducing indoleamine 2,3-dioxygenase. J Reprod Immunol. 2009; 80:1-11.
13. Munn DH, Zhou M, Attwood JT, Bondarev I, Conway SJ, Marshall B, Brown C, Mellor AL. Prevention of allogeneic fetal rejection by tryptophan catabolism. Science. 1998; 281:1191-1193.
14. Zenclussen AC, Gerlof K, Zenclussen ML, Sollwedel A, Bertoja AZ, Ritter T, Kotsch K, Leber J, Volk HD. Abnormal T-cell reactivity against paternal antigens in spontaneous abortion: adoptive transfer of pregnancy-induced $CD4^+$ $CD25^+$ T regulatory cells prevents fetal rejection in a murine abortion model. Am J Pathol. 2005; 166:811-822.
15. Ge YY, Zhang L, Zhang G, Wu JP, Tan MJ, Hu W, Liand YJ, Wang Y. In pregnant mice, the infection of *Toxoplasma gondii* causes the decrease of $CD4^+$ $CD25^+$-regulatory T cells. Parasite Immunol. 2008, 30:471-481.
16. Zhou ZW, Ji K, Zhu XY, Wu XY, Lin RT, Xie CC, Cai ZL, Chen JJ. Natural isoflavone formononetin inhibits IgE-mediated mast cell activation and allergic inflammation by increasing IgE receptor degradation. Food Funct. 2023; 14:2857-2869.
17. Jing W, Feng L, Peng K, Zhang W, Wang B. Formononetin attenuates osteoclast differentiation and calcium loss by mediating transcription factor AP-1 in type I diabetic mice. J Biochem Mol Toxicol. 2022; 36:e23042.
18. Jia C, Hu F, Lu D, Jin H, Lu H, Xue E, Wu D. Formononetin inhibits IL-1β-induced inflammation in human chondrocytes and slows the progression of osteoarthritis in rat model *via* the regulation of PTEN/AKT/NF-κB pathway. Int Immunopharmacol. 2022; 113:109309.
19. Li JY, Wang JX, Li QH, Li XF, Xiao J, Li SS, Shen XP, Zhang WD, Shen YH. Natural borneol enhances the anti-cerebral ischemia efficacy of formononetin in MCAO/R rats by promoting its delivery in the brain. J pharm pharmacol. 2022; 74:1598-1608.
20. Wang JY, Jiang MW, Li MY, Zhang ZH, Xing Y, Ri MH, Jin CH, Xu GH, Piao LX, Jin HL, Ma J, Jin Y, Zuo HX, Jin X. Formononetin represses cervical tumorigenesis by interfering with the activation of PD-L1 through MYC and STAT3 downregulation. J Nutr Biochem. 2022; 100:108899.
21. Yi L, Cui J, Wang W, Tang W, Teng F, Zhu X, Qin J, Wuniqiemu T, Sun J, Wei Y, Dong J. Formononetin attenuates airway inflammation and oxidative stress in murine allergic asthma. Front Pharmacol. 2020; 11:533841.
22. Shen L, Li Y, Hu G, Song X, Wang X, Li X, Xu X. Astragaloside IV suppresses the migration and EMT progression of cervical cancer cells by inhibiting macrophage M2 polarization through TGFβ/Smad2/3 signaling. Funct Integr Genomic. 2023; 23:133.
23. Shen Q, Fang J, Guo H, Su X, Zhu B, Yao X, Wang Y, Cao A, Wang H, Wang L. Astragaloside IV attenuates podocyte apoptosis through ameliorating mitochondrial dysfunction by up-regulated Nrf2-ARE/TFAM signaling in diabetic kidney disease. Free Radic Biol Med. 2023; 203:45-57.
24. Yang L, Han X, Yuan J, Xing F, Hu Z, Huang F, Wu H, Shi H, Zhang T, Wu X. Early astragaloside IV administration attenuates experimental autoimmune encephalomyelitis in mice by suppressing the maturation and function of dendritic cells. Life Sci. 2020; 249:117448.
25. Shao P, Zhao LH, Chen Z, Pan JP. Regulation on maturation and function of dendritic cells by *Astragalus mongholicus* polysaccharides. Int Immunopharmacol. 2006; 6:1161-1166.
26. Zhuge ZY, Zhu YH, Liu PQ, Yan XD, Yue Y, Weng XG, Zhang R, Wang JF. Effects of Astragalus polysaccharide on immune responses of porcine PBMC stimulated with PRRSV or CSFV. PLoS ONE. 2012; 7:e29320.
27. Chan DV, Gibson HM, Aufiero BM, Wilson AJ, Hafner MS, Mi QS, Won HK. Differential CTLA-4 expression in human $CD4^+$ versus $CD8^+$ T cells is associated with increased NFAT1 and inhibition of $CD4^+$ proliferation. Genes Immun. 2014; 15:25-32.
28. Tekguc M, Wing JB, Osaki M, Long J, Sakaguchi S. Treg-expressed CTLA-4 depletes CD80/CD86 by trogocytosis, releasing free PD-L1 on antigen-presenting cells. PNAS. 2021; 11:e2023739118.
29. Du MR, Dong L, Zhou WH, Yan FT, Li DJ. Cyclosporin a improves pregnancy outcome by promoting functions of trophoblasts and inducing maternal tolerance to the allogeneic fetus in abortion-prone mattings in the mouse. Biol Reprod. 2007; 76:906-914.
30. Wang S, Li M, Sun F, Chen C, Ye J, Li D, Qian J, Du M. Th17/Treg-cell balance in the peripheral blood of pregnant females with a history of recurrent spontaneous abortion receiving progesterone or cyclosporine A. Exp Ther Med. 2021; 21:37.
31. Wang T, Zhou Y, Wang K, Jiang X, Wang J, Chen J. Prediction and validation of potential molecular targets for the combination of *Astragalus membranaceus* and *Angelica sinensis* in the treatment of atherosclerosis based on network pharmacology. Medicine. 2022; 101:26 (e29762).
32. Wang T, Jiang X, Ruan Y, Li L, Chu L. The mechanism of action of the combination of *Astragalus membranaceus* and *Ligusticum chuanxiong* in the treatment of ischemic stroke based on network pharmacology and molecular docking. Medicine. 2022; 101:28 (e29593).
33. Wang T, Jiang X, Ruan Y, Zhuang J, Yin Y. Based on network pharmacology and *in vitro* experiments to prove the effective inhibition of myocardial fibrosis by Buyang Huanwu decoction. Bioengineered. 2022; 13:13767-13783.
34. Yousefzadeh Y, Soltani-Zangbar MS, Hemmatzadeh M, Shomali N, Mahmoodpoor A, Heris JA, Yousefi M. Fetomaternal immune tolerance: Crucial mechanisms of tolerance for successful pregnancy in humans. Immunol Invest. 2022; 51:1108-1125.

Received December 18, 2023; Revised February 13, 2024; Accepted February 16, 2024.

*Address correspondence to:
Kyoko Kobayashi, Division of Pharmacognosy, Faculty of Pharmaceutical Sciences, Tohoku Medical and Pharmaceutical University, 4-1 Komatsushima 4-Chome, Aoba-Ku, Sendai, Miyagi 981-8558, Japan.
E-mail: k-kyoko@tohoku-mpu.ac.jp

Released online in J-STAGE as advance publication February 21, 2024.